Egypt. J. Chem. **Vol. 66**, No. SI: 13 pp. 241 - 254 (2023)

Egyptian Journal of Chemistry

http://ejchem.journals.ekb.eg/

Green Hydrogen Gas Production Using an Adapted Electrolysis Method

Mohamed Mortada[1*], Yehia M. Youssef [2], I. Hassan[2], and Magdy A.M. Ibrahim[3]

[1] *Basic and Applied Science Institute, College of Engineering and Technology, Arab Academy for Science and Technology and Maritime Transport, Alexandria, Egypt*

[2] *Department of chemical and petrochemical Engineering, College of Engineering and Technology, Arab Academy for Science and Technology and Maritime Transport, Alexandria, Egypt*

[3] *Department of chemistry, Faculty of Science, Ain Shams University, Cairo, Egypt*

Abstract

An electrolysis cell for hydrogen gas production was constructed in the form of a fixed bed. The electrodes were made from 316L stainless steel in the form of cylinders 15 mm in height and diameter (aspect ratio = 1). The electrodes were immersed in an aqueous solution of 1 M, 1.5 M, and 2 M sodium hydroxide. Both anodic and cathodic solutions were pumped from a 30-liters stainless steel storage tank by two plastic pumps. Flowrate was varied during the experiments between 1,2, and 3 liters/min. The cathodic and anodic compartments were separated by a cation exchange membrane (Fumasep E-620-K). The membrane is characterized by a non-reinforced, small thickness of 20µm, with very low resistance, high selectivity, and high stability in different pH environments. Using cylindrical electrodes allowed to maximize of the surface area on each side of the cell with the same NaOH concentration. The effect of current density was investigated by conducting experiments at, 4 mA/cm^2, 6 mA/cm^2, and 8 mA/cm^2. The temperature was also varied (55 ^{o}C, 65 ^{o}C, and 75 ^{o}C) which resulted in an increase in the cell efficiency from 8.3% to 81.5%. The present study investigates the effect of different variables on cell performance. The different variables investigated included: solution concentration, current density, solution flow rate, and temperature. The resulting flow rate of produced hydrogen gas, the effect of electrolyte solution volume, and cell voltage were evaluated. The produced oxygen gas, power consumption, energy consumption, and ampere hour capacity are calculated, and the cell efficiency is therefore evaluated by comparing the theoretical and experimental mass flow rates of hydrogen gas. Additionally, the characterization of electrodes before and after the experiment was done using scanning electron microscopy (SEM) examination and alloy composition elemental Mapping.

keywords: Hydrogen production; a fixed bed electrochemical reactor; and water electrolysis

1. Introduction

In recent years, the global population and standard of life have expanded resulting in a progressive growth in energy consumption. Moreover, as global warming and pollution intensified the importance of developing renewable energy sources grew. Hydrogen is one of the most promising clean and sustainable energy carriers since it emits no carbon dioxide and produces only water as a byproduct [1]. Hydrogen has a high energy density (140 MJ/kg) which is more than twice that of ordinary solid fuels (50 MJ/kg). This is one of the many enticing qualities of hydrogen as an energy carrier. The current global output of hydrogen is anticipated to exceed 500 billion cubic meters per year. The created hydrogen is utilized in numerous industrial applications including fertilizers, petroleum refining, petrochemical, fuel cell, and chemical industries. Hydrogen has been produced from a variety of renewable and non-renewable energy sources, including fossil fuels, particularly steam reforming of methane, coal gasification, biomass, and geothermal energy [2]. Additionally, the ever-increasing global energy demands coupled with limited fossil fuel supplies, sustainability, and environmental impact necessitate the development of carbon-free energy innovations. Today, there is a great deal of emphasis on ecologically friendly energy systems that may be able

*Corresponding author e-mail: m.mortada3649@aast.edu; (Mohamed Mortada)

EJCHEM use only: Received 12 December 2022; revised 12 February 2023; accepted 06 March 2023

DOI: 10.21608/EJCHEM.2023.175880.7323

to replace the present energy production based on fossil fuels. This can be achieved through the production of hydrogen from replenishable water. Water splitting and electrolysis are ecologically benign and high-purity (99.999%), hydrogen manufacturing technologies that employ water to produce pure hydrogen and oxygen via thermal, electrolytic, photolytic, and chemical conversion of biomass water splitting. Due to its widespread availability water is considered a sustainable feedstock for hydrogen production. The production of hydrogen from water has the potential to significantly reduce the depletion of fossil fuels and CO_2 emissions [3-6].

However, because of the high energy consumption and low hydrogen evolution rate, the efficiency of hydrogen synthesis via water electrolysis is insufficient for economic viability. As a result, a large number of academics have been creating alternative low-cost, high-efficiency, energy-saving technologies to increase efficiency, and reduce energy, and power consumption. Water electrolysis is a well-developed process for converting water into hydrogen and oxygen at low temperatures and accounts for 4% of global hydrogen production with a cost-effective method of energy storage and transfer. Using various electrode materials and membrane separators between the anode and cathode compartments, scientists continue to improve the overall system efficiency. Alternative couplings, storage mediums, and membrane assemblies for electrolyzers are being developed to increase efficiency. A method for determining the efficiency of hydrogen-generating systems has been proposed. Hydrogen production using photo-electrocatalysis is another intriguing method for creating hydrogen from water. Here, solar energy is converted into chemical energy.

Electrolysis can be identified by the type of electrolyte utilized in the electrolyzer. Alkaline electrolysis and proton exchange membrane (PEM) electrolysis are the two most important methods for creating hydrogen via water electrolysis. In alkaline water electrolyzers with narrow gaps, electrodes are pressed near porous separators loaded with liquid NaOH or KOH electrolytes for alkaline electrolysis. Two advantages of this technique are the use of inexpensive metals like Fe for cells, system components, and a disposable electrolyte. However, greater resistances are associated with disadvantages, primarily thick separators and intense electro-catalytic reactions at high voltages. Acidic water electrolyzers with thin polymer electrolyte membranes are widely advised for increasing current densities, and efficiency and reducing power consumption because they are less susceptible to mass transport limitations. It has been demonstrated that hydroelectric power is the most potential renewable energy source for manufacturing hydrogen, using a variety of approaches to link electrolyzers with various renewable energy sources to determine the most efficient system. In addition, the type of membrane and electrolytes employed can substantially affect the reactor's functioning [7]. Electro-membrane activities like electro-dialysis, diffusion dialysis, energy conversion, and energy storage have generated considerable interest in ion exchange membranes (IEMs). It's approved that using a membrane instead of an acrylic separator enhanced the efficiency of hydrogen production. The three types of IEMs are anion exchange membranes (AEM), cation exchange membranes (CEM), and bipolar membranes (BPM). In the electrolysis process AEMs and CEMs are commonly used to create chlorine and caustic soda or hydrogen and oxygen respectively. Additionally, IEMs are crucial components in fuel cell and energy storage devices such as batteries [8-10].

The previous studies focused on the synthesis of hydrogen chemically and electrochemically via different technologies with the addition of a catalyst which enhances the production rate of hydrogen gas. Recently, sustainable H_2 can be produced on a lab scale using a copper-chlorine cycle with a rate of up to 100 L/h. Using $Bi_2(CrO_4)_3$ by photocatalytic water splitting produced 522.44 and 88.24 μmol/g/h of H_2 under UV and visible irradiations. a new reactor fabricated using solar energy as an energy source and aluminum metal, a maximum H_2 production rate and reactor coefficient of performance was 420 mL/min and 1261 ml H_2 per 1 g of Al respectively. Electrolysis by HI solution ($HI-I_2-H_2O$) produced about 300 ml H_2 after 1 hour. H_2 production through a thermochemical water sulfur–iodine splitting cycle using hydriodic acid, They used several commercial proton-exchange membranes (PEMs) and reported that about 700 and 300 ml H_2 can be generated for 100 and 50 mA cm^{-2} current densities at 60 ◦C respectively [11]. A new study has been investigated to observe the contribution of the design and thermal characterization of an alkaline electrolysis cell for hydrogen generation at atmospheric pressure, The electrolytic cell was manufactured from acrylic, 316 L stainless steel sheets as electrodes and considering a membrane separation for gases, the effect of current conditions, the distance between electrodes on the production efficiency of hydrogen, the distribution and variation of temperatures on the surface of the electrodes in operation were evaluated, Maximum hydrogen generation was achieved with a separation between electrodes of 3 mm and a current of 30 A at 12 V. The performance of an alkaline electrolysis cell for the application of remote area hydrogen using photovoltaic panels, maximum efficiencies of

31%was achieved for the alkaline electrolysis cell and 4.6% for the entire system including a 360 W solar panel [12].

Water electrolysis offers high production of hydrogen but due to slow reaction rates on many electrode surfaces, electrocatalysts needed such as platinum, Nickel and rhenium[13], may be impractical for economic operation. Therefore, research in this area has been focused on finding materials that can replace these expensive electrocatalysts. The electrocatalytic behavior of stainless steel 304L and 316L towards water dissociation owing to its availability and comparatively inexpensive. Results of microscopic characterization, the crystallographic orientations, the catalytic activity, and long-term stability of stainless steels have yielded results similar to or sometimes better than those of the noble electrocatalysts, the possible research to find solutions to overcome existing challenges is needed like lack of active centers, the surface modification needed, poisoning of active reaction centers, lower operating current density, cell efficiency, and overall low stability, the solution to which could make stainless steel a viable replacement for the precious metals electrocatalysts [14-16]. The thickness of the diaphragms can be reduced with lower resistance this can improve the cell efficiency, increase the current density with high specific surface area electrode materials, reduce the electricity consumption and reduce this crossover of the gasses observed at the highly concentrated KOH electrolyte using a high thickness of diaphragms with nickel-based electrodes. this would improve cell efficiency from 53% to 75% at 1 A/cm^2 [15]. Also, membrane durability is one of the major challenges. Generally, the membrane's durability is around 30,000 h only due to the polymer degradation from the membrane backbone chain. Therefore, considerable innovations are required to increase the durability and overcome polymer degradation which can be achieved by increasing the chemical, mechanical, and thermal stability of the membranes along with increasing the ionic conductivity using high-conducting polymer compositions [14, 15]. The nominal current density is typically selected based on a trade-off between the capital and operational costs of an electrolyzer. A lower nominal current density results in better efficiency of the plant reducing electricity costs but means that more electrolyzers are needed to make the same amount of hydrogen, resulting in higher capital costs. In practice electrolyzer systems typically have a nominal current density corresponding to an efficiency of 75–80% (based on the higher heating value of hydrogen), which corresponds to a cell potential of 1.85–1.97 V [17].

Recent BPMs are produced using plasma-induced polymerization, their performance is evaluated by monitoring the cell voltage and H_2 production rate as a function of current densities for cells with and without BPMs. It has been discovered that BPMs as diaphragms increase the hydrogen production efficiency of the cell. AEMs can be employed in electrochemical applications, including fuel cells [18, 19], due to their ability to function in low-temperature fluids and utilize non-precious metals as catalysts. The diffusion mechanism is the most prevalent transport mechanism in AEMs, it carries OH^- across the membrane surface. In an AEM electrolysis reactor, the cathode and anode comprise the external circuit that supplies DC electricity. In an alkaline electrolyte, the internal circuit is separated by the AEM. Thus, on the anode side, the half-reaction generates water and oxygen (OER) where the hydroxyl ions (OH^-) are discharged to produce 0.5 mole of oxygen (O_2) and one mole of water (H_2O). On the cathode side, the hydrogen network link breaks to produce hydrogen ions (HER) where two moles of alkaline solution are reduced to produce one mole of hydrogen (H_2) and two moles of hydroxyl ions (OH^-), and created on the electrode surface via electron transfer. Half-reactions occur when the applied potential is larger than the Gibbs free energy. Due to ohmic resistance and the need to overcome the kinetics of the electrolyte, the minimum applied potential needed in practice is more than the theoretical minimum. Under normal working conditions, the minimum applied potential is frequently greater than 1.85 V [20-22].cost estimates across all experts for all three electrolyzer types in 2020. Capital costs for AEC systems by 2020 lie between 800 and 1300 $/kW. For PEMEC the respective range is 1000 to 1950 $/kW. SOEC electrolyzers are estimated to be most expensive at 3000 to 5000 $/kW, at 2030 the cost expected to be reduced [23]

2. Experimental Methods

2.1. Materials

Both anolyte and catholyte solutions are solutions of varying concentrations of Sodium hydroxide (1 M, 1.5 M, and 2 M) prepared with distilled water and solution concentration calibrated using a spectrophotometer DR-3900.

2.2. Measures and analysis

The suggested cell, as depicted in figure (1), was constructed as a fixed-bed cell. The electrodes from stainless steel 316L as cylinders 15 mm in height and 15 mm in diameter (aspect ratio = 1) are immersed in an aqueous solution of 1 M, 1.5 M, 2 M sodium hydroxide as anode solution and a cathode solution pumped from 30-liter stainless steel storage by two

plastic pumps at varying flow rates of 1, 2, and 3 liter per minute, while the two half cells are separated by a cation exchange membrane Fumasep E-620-K. To increase cell efficiency, we maximized the electrode area to 757,045 cm^2 on each side and employed the same concentration of sodium hydroxide at 55^oC, 65^oC, and 75^oC with varying current densities of 4 mA/cm^2, 6 mA/cm^2, and 8 mA/cm^2, distance between electrodes was 1.0 cm from each other and 0.5 cm to the membrane. This study's outline is based on cell performance in terms of solution concentration, current density, flow rate, temperature, measurement of the volumetric flow rate of produced hydrogen gas (ml/min), reduction in electrolyte solution volume of 30 liters, and cell voltage. The percentage of oxygen gas produced, power consumption, energy capacity consumption, ampere-hour capacity consumption, and cell efficiency are calculated by comparing the theoretical and experimental mass flow rate of evolved hydrogen gas. Additionally, the characteristics of electrodes using SEM and Mapping of alloy components ensure that cathodic metal is unaffected while the anodic one has tiny pits on the protective oxide under the effect of stress corrosion cracking, as depicted in figure (2). Concentration of dissolved Fe^{+2} was tested by using a spectrophotometer DR-3900 and atomic absorption spectroscopy and it's not exceeded 0.05 mg per liter. Produced hydrogen gas purity was tested by gas chromatography.

Cell responses[24]

At the cathode: two moles of alkaline solution are reduced to produce one mole of hydrogen and two moles of hydroxyl ions on the surface of stainless steel.

$$4H_2O + 4e^- = 2H_2 + 4OH^- E^o = -0.828\ V \quad (1)$$

While at the anode: the two hydroxyl ions are discharged to produce the 0.5 mole of oxygen (O_2) and one mole of water on stainless steel in the presence of sodium hydroxide solution

$$4OH^- = O_2 + 2H_2O + 4e^- E^o = 0.4V \quad (2)$$

Total cellular response:

$$2H_2O = 2H_2 + O_2 E^o = 1.23V \quad (3)$$

Experiments were conducted utilizing the apparatus depicted in Figure (1) for measurements and analysis. The reactor contains four sections which are the inlet, the outlet sections for the electrolyte solution, the Upper outflow section for hydrogen and oxygen gases, the electrical circuit, and the working portion. The working portion of the reactor is comprised of two 15x15x15 cm^3 translucent plexiglass cubes with a thickness of 10 mm, the input and output parts are comprised of plastic pipes with stainless steel 316L valves to control the flow rate and a flow meter to measure the electrolyte's volumetric flow rate. While the two cubic compartments separated by a cation exchange membrane (Fumasep E-620-K) that only permits the passage of sodium ions and prohibits the passage of hydroxide ions and is characterized by small thickness (20µm) to reduce resistance, facilitate and improve ionic conductivity. The anodic compartment consists of a sheet of stainless steel 316L (10 cm x 10 cm) directly connected to stainless-steel 316L cylinders (1.5 cm height x 1.5 cm diameter) with an aspect ratio = 1 with a total area of 757.045 cm^2 that are connected and to the positive pole of a DC power supply to function as an anode and immersed in different concentrations of sodium hydroxide solution. The cathode compartment is comprised of a stainless-steel 316L sheet (10 cm x 10 cm) and stainless-steel 316L cylinders (1.5 cm height x 1.5 cm diameter)) with an aspect ratio = 1 and a total area of 757.045 cm^2, connected to the negative pole of the DC power supply to function as a cathode and immersed in the same sodium hydroxide electrolyte solution. The solution is heated using a stainless-steel 316L coil as a heater within the tank with temperature control and pumped from stainless-steel 316L storage tanks at various temperatures 55 ^oC, 65 ^oC, and 75 ^oC to the two half cells using Iwaki plastic centrifugal pumps with half horsepower. The electrical circuit was comprised of a 40-volt and 10-ampere direct current power source, a multi-range ammeter linked in series with the cell, and a high-impedance voltmeter connected in parallel to monitor the cell voltage. Before each run, a plastic centrifugal pump circulates the solution from the storage tank to the two half-cells. The solution entered the half-cell via the intake tube positioned above the cell's base. An identical pair of exit tubes for each side were installed at the reactor's apex. The solution flow rate is controlled by stainless steel 316L valves, and the current was adjusted to the required value using a variable rheostat. Hydrogen and oxygen gas are then produced and collected over the surface of the solution, before entering the upper section, which is responsible for separating water vapor from evolved gases by condensation (using a condenser and an ice path surrounding the upper column). Evolved gases pass through the non-return valve (prevent gas from the return to the working portion) and then to the gas flow meter to identify the volume of produced hydrogen and oxygen and pressure gauge to identify the pressure of evolved hydrogen and oxygen.

3. Results and Discussion

3.1. Relationship between hydrogen production rate, voltage and time:

The study show that the cell voltage decreases slightly with increasing time (decreased by 0.1 to 0.3 volt over 100 minutes concerning other variables) where the average maximum cell voltage at current densities of 4 mA/cm^2, 6 mA/cm^2, and 8 mA/cm^2 respectively reach 3.9 V, 5.3 V, 5.9 V at lower concentration, temperature conditions and the average minimum cell voltage at reach 2.2 V, 3.3 V, 4.2 V at higher concentration and temperature conditions at the same current densities. while as shown in Figure (3) the flow rate of produced hydrogen increases gradually in the first 30 minutes and then becomes constant till the end of each run, since electrolysis of water in standard conditions requires a theoretical minimum of 237 kJ per mole of electrical energy to dissociate each mole of water, which is the standard Gibbs free energy of formation of water and energy to overcome the change in entropy of the reaction. Therefore, the process cannot proceed below 286 kJ per mole if no external energy is added, it follows that the minimum voltage necessary for electrolysis is about 1.23 V, but If electrolysis is carried out at a high temperature, this voltage reduces. In this way, thermal energy can be used for part of the electrolysis energy requirement which improves the diffusion of electroactive species till reaches a constant reaction rate. indicating that all electrons provided by the negative pole of the DC power supply to the cathode are consumed by a large number of hydrogen ions [24-26].

$$\Delta G^0 = \Delta H^0 - T\Delta S^0 = -nFE^0 \quad (4)$$

The primary sources of increased voltage over reversible potential which corresponds to a zero-reaction rate may include ohmic loss of electrolyte, ohmic loss for electric resistance of electrodes, circuitry, and overvoltage associated with oxygen and hydrogen reactions. Both overvoltage and ohmic loss increase with the increasing current density [27].

3.2. Effect of the flow rate:

As shown in Figure (4), the flow rate of produced hydrogen increases. Also increases from 23.9 ml/min, 30.9 ml/min to 38.7 ml/min as the flow rate of the electrolyte solution increases from 1 L/min, 2 L/min to 3 L/min (Laminar flow) with respect to other parameters, as a result of increasing the rate of mass transfer of the ions to the electrode surface, reduce the thickness of the diffusion layer or boundary layer and removing bubbles from the electrodes surface under different current densities either by stirring or by pumping the solutions at higher velocities through each half-cell at a faster rate. It observed that At low current density, the increase in electrolysis potential caused by bubbles is not obvious, the H_2 and O_2 bubbles in the gas-evolving electrodes result in a substantial effect on mass and heat transfer, But when the current increasesmore bubbles cause a slight increase in electrolysis potential[28]. Electrolyte solution must be isolated from the surrounding atmosphere to avoid the effect of carbon dioxide, which reacts with a caustic solution to generate carbonates, which reduce the conductivity of electrolyte solution (consume hydroxyl groups), block membrane, forming scale and decrease electrolysis efficiency [29, 30].

3.3. Implications of current density:

As depicted in Figure (5), the produced hydrogen gas flow rate increases by increasing the current density. Also increases from 33.4 ml/min, 36.4 ml/min to 38.7 ml/min. with increasing the current density from 4 mA/cm^2, 6 mA/cm^2, to 8 mA/cm^2 tends to increasing the amount of consumed electricity (more electrons) on the metal surface, which attracts more hydrogen ions on the cathode and increases the rate of hydrogen and oxygen gas production. Increasing current density tends to accelerate the rate of electrochemical reaction, resulting in a greater hydrogen gas production rate. However, it has been observed that at higher current densities, the number of gas bubbles on the electrode surface increases (removed under the effect of electrolyte pumping) thereby increasing the electrolysis potential which is not obvious at low current density [25, 28, 29].

$$m = Z\,I\,t \quad (5)$$

m = mass of a substance (in grams) deposited or liberated at an electrode, z is the proportionality constant or electrochemical equivalent grams per coulomb (g/C), t is the time in a second, and I represent the total current in ampere.

3.4. Concentration's effects:

As demonstrated in Figure (6), the produced hydrogen flow rate increases with increasing concentration. Also increases from 29.5 ml/min, 35.7 ml/min to 38.7 ml/min. Increasing the concentration of sodium hydroxide solution from 1 M, 1.5 M to 2 M causes a reduction in the effect of concentration polarization, a higher diffusion rate of ions to the counter electrode, an increase in ionic conductivity, a decrease in electrolyte resistivity, a higher number of the available reactant at the electrode surface area for reaction at same power input, reduce cell voltage and an increase in the electrical current passing through the solution and consequently to a decrease of the requirement of less voltage at same current density

operation which leads to increase in hydrogen and oxygen production efficiency [27] concerning the purity of distilled water and exposure to moisture to avoid blocking of active reaction sites on metal surface and membrane. Also, it is observed that voltage decreases with increasing the electrolyte concentration, this is due to reduce cell resistance [24, 30, 31].

3.5. The impact of temperature:

As illustrated in Figure (7), the production rate of hydrogen gas increases. Also increase from 33.6 ml/min, 36.7 ml/min to 38.7 ml/min. By increasing the temperature of the electrolyte solution from 55 ^{o}C, 65 ^{o}C, to 75 ^{o}C, it was discovered that increasing the temperature helps to maximize the diffusion of ions, decrease the cell voltage, reducing the system's energy requirements from 58.5 Wh, 56.8 Wh to 55.9 Wh by increasing the temperature of the electrolyte solution from 55 ^{o}C, 65 ^{o}C, to 75 ^{o}C at 8 mA/cm^2 (lowering Gibb's free energy and cell performance increases with temperature due to reduced reversible potential, kinetic loss, and ohmic loss) [27], minimizing cell resistance, accelerating the rate of electrochemical reaction, decreasing the activation overpotential [24, 25, 32]. Temperature is one of the most important variables in electrolysis because the efficiency increases with increasing the temperature due to the required potential to produce the same quantity of hydrogen being reduced considerably, causing the cell more efficient, since it needs fewer energy requirements. This behavior is due to the rupture potential of a molecule decreasing with increasing temperature. This is explained, through the mass transfer phenomena that occur in the electrolyzer, since an increase in temperature favors the molecular collisions between ions of the electrolyte. A high number of molecular collisions facilitates the passage of an electric current through the electrolyte. Hence, higher temperature help to facilitate the stretching of the OH bands, and less amount of energy is needed to break the OH for hydrogen production, the electrical resistance decreases (ionic conductivity of the electrolyte increases) which increasing the efficiency of the electrolytic cell [33].

3.6. Relationship between energy use (power consumption), consumed ampere hour capacity, energy density consumption against temperature and the rate of hydrogen production:

$$P\ (W) = I\ (mA/cm^2) \times V\ (volts) \quad (6)$$

As demonstrated in Figures (8), the production rate of hydrogen and oxygen gas increases. Its rises from 24.2 ml/min, 26.7 ml/min to 29.5 ml/min by increasing electrolyte temperature and power consumption decreases from 35.3 W, 34.2 W to 33.7 W by increasing the temperature of the electrolyte solution from 55 ^{o}C, 65 ^{o}C, to 75 ^{o}C at constant current density. To minimize the resistance and power loss, the membrane must have a high ionic conductivity, and hydrophilic characters at the interface between the liquid electrolyte and solid membrane surface to ensure a fast ion transfer. In addition, the fast ionic transport must be highly selective and the transport of active species must be minimized to reduce energy losses [4, 29].

$$(Ah) = I_{total}\ (Ampere) \times (t)\ (hours) \quad (7)$$

As seen in Figures (9), the production rate of hydrogen and oxygen gas rises. The ampere-hour capacity will remain constant unless the current density is increased, at which point it will increase from 4.98 Ah to 7.47 Ah to 9.96 Ah with increasing current density from 4 mA/cm^2, 6 mA/cm^2, to 8 mA/cm^2 which means increasing the electrolysis current made the current (ampere) consumption by active species with respect to time increase which leads to higher production rate of hydrogen (14.1 ml/min to 16.5 ml/min to 18.9 ml/min at 55 ^{o}C, 16.1 ml/min to 18.7 ml/min to 21.3 ml/min at 65 ^{o}C and 18.5 ml/min to 21.5 ml/min to 23.9 ml/min at 75 ^{o}C) but with reduced electrolysis efficiency [29, 34].

$$E\ (KWh) = V\ (volts) * I_{total}\ (A) * t\ (minutes) \quad (8)$$

As demonstrated in Figures (10) the production rate of hydrogen and oxygen gas increases. Increasing the temperature maximizes the diffusion of ions and decreases the cell voltage, while other variables directly affect the energy density consumption reduced from 111 kWh/kg of H_2, 89.4 kWh/kg to 75.6 kWh/kg at 4 mA/cm^2 by increasing the temperature of the electrolyte solution from 55 ^{o}C, 65 ^{o}C, to 75 ^{o}C at 8 mA/cm^2 and 302.3 kWh/kg, 266.1 kWh/kg, 236.8 kWh/kg at the same current densities, where it is found to decrease with increasing electrolyte temperature due to a reduction in cell voltage, decreases system energy requirements at constant current density [4].

3.7. Effect of concentration and temperature on cell voltage

As shown in Figure (11,12), as concentration and temperature (important parameters and responsible for determining system efficiency) increased, the cell voltage decreased from 5.88 V, 5.64 V to 5.1 V at 8 mA/cm^2. This was caused by an increase in concentration reducing the effect of concentration

polarization, a higher diffusion rate of ions to the word electrode, a rise in ionic conductivity, and a decrease in electrolyte resistivity. Increasing the temperature maximizes the diffusion of ions and reduces the cell voltage from 3.9 V, 3.8 V to 3.7 V by increasing the temperature of the electrolyte solution from 55 ^{o}C, 65 ^{o}C, to 75 ^{o}C at 4 mA/cm^2 with regard to other variables where increasing the temperature reduces the system energy requirements, minimizes cell resistance, improves hydroxyl group conductivity, accelerates the rate of electrochemical reaction, resulting in a higher hydrogen gas production rate, and reduces the activation over potential [25, 29, 33].

3.8. Effect of current density on cell voltage

As demonstrated in Figure (13), as current density increases, more electrons are transferred, the rate of electrochemical reaction increases, and the cell voltage rises from 3.7 V, 5.03 V to 5.6 V with increasing current density from 4 mA/cm^2, 6 mA/cm^2, to 8 mA/cm^2 at 75 ^{0}C due to constant cell resistance [29].

The hydrogen production rate increase with increasing voltage because of the lowering in bonding energy of hydrogen and oxygen. Therefore, increasing the temperature, the enthalpy of the system increase, larger number of molecules get high energy as voltage and temperature increase where the OH bonds easily stretched and the interaction between OH decreases and less amount of energy is needed to break the OH bond therefore the production of hydrogen with temperature and voltage are directly proportional [35]. At a low current density, the operating voltage increases by the activation overpotential which can be reduced by the addition of a catalyst, at the mid-level current density, the operating voltage increases owing to the ohmic loss, at a high current density, the operating voltage increases owing to the mass transfer parameters [36].

3.9. Cell performance and system effectiveness:

Depending on the operating conditions and measured parameters, the electrolysis efficiency can be computed in a variety of ways, in the present work the faradic efficiency will be calculated using the experimental (actual) and theoretical mass flow rates of produced hydrogen gas. Improvements in efficiency are possible but not prioritized for two reasons. First, relatively low electricity costs and non-continuous operation, operating costs are small, so the reduction of capital costs has priority. Second, efficiencies are maximized at low current density, but to reduce capital costs, however, most research is focused on increasing current density. Experts also highlight that system efficiency alone is not the most important factor, but rather the efficiency including hydrogen purification and pressure- isolation for its final application [23].

*% Electrolysis Efficiency = (actual mass flow rate of hydrogen gas collected/theoretical mass flow rate of hydrogen) * 100. (9)*

At low pressure and temperature, hydrogen gas can behave as an ideal gas. The electrolyzer records efficiencies ranging from 8.3% to 81.5%, depending on the operating conditions of current density, temperature, electrolyte solution concentration, and flow rate as shown in figure (14,15,16,17), the cell efficiency increased from 58.8%, 76.9% to 81.5% by increasing the concentration due to increase the concentration reduces the effect of concentration polarization, the higher diffusion rate of ions to the word electrode, and increasing the ionic conductivity. Increasing current density tends to accelerate the rate of electrochemical reaction, resulting in a greater hydrogen gas production rate with lower efficiency 81.5%, 61.5% to 50.9% with increasing current density from 4 mA/cm^2, 6 mA/cm^2, to 8 mA/cm^2, therefore current density is regarded as a crucial parameter governing system efficiency [29].

The higher efficiencies value (81.5% and 76.9%) appears at higher concentrations of 2 M and 1.5 M at temperature 75 ^{0}C and smaller current density of 4 mA/cm^2 and reaches, whereas the lower values (8.3%) appear at lower flow rates of electrolyte solution, indicating the significant effect of pumping electrolyte solution on the rate of mass transfer and rate of hydrogen production. The cell efficiency is mediated between 20%-80%, which is comparable and accepted values compared with others as shown in table (1) [37-43].

4. Conclusions:

Based on the outlined data in the present study, several important points can be concluded and listed. The cell voltage decreases with time by 0.1 to 0.3 volts per 100 minutes (time of each run). The hydrogen production rate increases from 4.2 ml/min to 38.7 ml/min as the electrolyte solution flow rate, current density, concentration, and temperature of sodium hydroxide solution are increased.

Elevation of electrolyte temperature reduces power consumption from 35.2 watts to 6.7 watts, and energy density consumption is reduced from (302.3 kWh/kg of H_2 to 75.6 kWh/kg of H_2) owing to voltage reduction at constant current density. While Ampere-hour capacity consumption is constant over all cycles unless the current density is increased. With increasing current density from 4 mA/cm^2, 6 mA/cm^2 to 8 mA/cm^2, the ampere-hour capacity consumption begins to increase from 4.98 Ah to 7.47 Ah to 9.96 Ah.

Higher efficiencies of 81.5% are observed at higher concentrations, temperatures, and flow rates, while lower efficiencies of 8% are observed at lower flow rates of electrolyte solution and current density, indicating that electrolyte solution pumping has a significant effect on the rate of mass transfer and the rate of hydrogen production.

5. Conflicts of interest

The results of this study may be extended to explore further evaluation points according to the following recommendations. Change the shape of the electrode to a hollow cylinder, use a vibrated electrode, addition of catalyst, and use multiple stacks.

6. Formatting of funding sources

There are no funding sources.

7. References

1. Turner J, S.G., Mann MK, Maness P-C, Kroposki B, Ghirardi M, Evans RJ, Blake D. , *Renewable hydrogen production.* . Int J Energy Res 2008. **32**(5): p. 379-407.
2. Acar C, *Evaluation of a new continuous type hybrid photo-electrochemical system.* . Int J. Hydrogen Energy 2015. **40**(34): p. 11112-11124.
3. Dincer I, B.M., *Potential thermochemical and hybrid cycles for nuclearbased hydrogen production.* Int J Energy Res 2011. **35**: p. 123-137.
4. Dincer I, Z.C., *Sustainable hydrogen production options and the role of IAHE.* Int J Hydrogen Energy 2012. **37**: p. 16266-16286.
5. Tufa RA, R.E., Chanda D, Hnat J, van Baak W, Veerman J, et al, *Salinity gradient power-reverse electrodialysis and alkaline polymer electrolyte water electrolysis for hydrogen production.* J Membr Sci 2016. **514**: p. 155-164.
6. Wang AQ, L.Y., Xu B, Hu CY, Xia SJ, Zhang TY, et al, *Kinetics and modeling of iodoform degradation during UV/chlorine advanced oxidation process.* . Chem Eng J 2017. **323**: p. 312-319.
7. Ogungbemi E, I.O., Khatib FN, Wilberforce T, El Hassan Z, Thompson J, et al *Fuel cell membranes e pros and cons.* . Energy 2019. **172**: p. 155-172.
8. H, S., *Ion-exchange membrane processes: their principle and practical applications. first ed. Hopkinton: Desalination Publications*. 2016: Hopkinton.
9. Weng G-M, L.C.-Y., Chan K-Y, *Three-electrolyte electrochemical energy storage systems using both anion- and cation-exchange membranes as separators.* Energy 2019. **167**: p. 1011-1018. .
10. Mahmoud Gamal Saleh, S.A.E.W., Syed K Noustafa 3, *Catalytic Activity of Modified Electrodes in Fuel Cells. I. The Electrochemical Behavior of Rhenium under Natural Corrosion Conditions.* Egyptian Journal Of Chemistry, 2020. **63**(10): p. 3607-3618.
11. Sohrab Zendehboudi, *A comprehensive review on hydrogen production and utilization in NorthAmerica: Prospects and challenges.* Energy Conversion and Management 2022. **269**: p. 115927.
12. Alcántar-Camarena, V., *Thermal characterization of an alkaline electrolysis cell for hydrogen production at atmospheric pressure.* Fuel, 2020. **276**: p. 117910.
13. Abdel-karim, A.A.M.R.M., *Electrocatalytic Activities of Macro- Porous Nickel Electrode for Hydrogen Evolution Reaction in Alkaline Media.* Egyptian Journal Of Chemistry, 2019. **62**(4): p. 665-678.
14. W. Haidera, *A review on the electrocatalytic dissociation of water over stainless steel: Hydrogen and oxygen evolution reactions.* Renewable and Sustainable Energy Reviews 2022. **161**: p. 112323.
15. Lima, H., *An overview of water electrolysis technologies for green hydrogen production.* Energy Reports 2022: p. 13793-13813.
16. Nady Hashem, E.S.G., Mohammed EL-Rabiei, Ahmed A. Bahrawy, *Electrochemical Performance of Fe-Cr-Ni Electrode as Cathode for Hydrogen Evolution in KOH Solutions.* Egyptian Journal Of Chemistry, 2021. **64**(9): p. 5037-5043.
17. Groot, M.T.d., *Optimal operating parameters for advanced alkaline water electrolysis.* International Journal of Hydrogen Energy, 2022. **47**(82): p. 34773-34783.
18. Danks TN, S.R., Varcoe JR, *Alkaline anion-exchange radiation-grafted membranes for possible electrochemical application in fuel cells.* J Mater Chem 2003, 13,, 2003. **13**: p. 712-721.
19. Li Y, Z.B., Zheng G, Liu X, Li T, Yan C, et al, *Continuously prepared highly conductive and stretchable SWNT/MWNT synergistically composited electrospun thermoplastic polyurethane yarns for wearable sensing.* J Mater Chem C, 2018. **6**: p. 2258-2269.
20. Grew KN, C.W., *A dusty fluid model for predicting hydroxyl anion conductivity in alkaline anion exchange membranes.* J Electrochem Soc, 2010. **157**(3): p. 327.
21. Hibbs MR, H.M., Alam TM, McIntyre SK, Fujimoto CH, Cornelius CJ, *Transport properties of hydroxide and proton conducting membranes* Chem Mater, 2008. **20**: p. 2566-2573.
22. Ito H, K.N., Someya S, Munakata T *Pressurized operation of anion exchange membrane water electrolysis.* Electrochim Acta, 2019. **297**: p. 188-196.
23. Schmidt, O., *Future cost and performance of water electrolysis : An expert elicitation study.* International Journal of Hydrogen Energy, 2017. **42**: p. 30470-30492.
24. Leng Y, C.G., Mendoza AJ, Tighe TB, Hickner MA, Wang C-Y, *Solid-state water electrolysis with an alkaline membrane.* J Am Chem Soc 2012, 2012. **134**: p. 9054–9057.
25. An L, Z.T., Chai ZH, Tan P, Zeng L. , *Mathematical modeling of an anionexchange*

membrane water electrolyzer for hydrogen production. Int J Hydrog Energy 2014. **39**: p. 19869–19876.
26. Pavel CC, C.F., Emiliani C, Santiccioli S, Scaffidi A, Catanorchi S, et al, *Highly efficient platinum group metal free based membrane-electrode assembly for anion exchange membrane water electrolysis.* Angew Chem Int Ed, 2014. **53**: p. 1378–1381.
27. opu, M.S., *Effect of Operating Parameters on Performance of Alkaline Water Electrolysis.* Int. j. of Thermal & Environmental Engineering 2015. **9**(2): p. 53-60.
28. H.Vogt, *On the mechanism of the anode effect in aluminum electrolysis.* Journal of Metallurgical and Materials Transactions B, 2000. **31**: p. 1225-1230.
29. Larminie J, D.A., *Fuel cell systems explained*. 2nd ed. 2013, New York: Wiley.
30. Naughton MS, B.F., Kenis PJA, *Carbonate resilience of flowing electrolytebased alkaline fuel cells.* J Power Sources, 2011. **196**: p. 1762–1768.
31. Prestat, M., *Corrosion of structural components of proton exchange membrane water electrolyzer anodes: A review.* Journal of power sources, 2023. **556**: p. 232469.
32. Ahn SH, L.B.-S., Choi I, Yoo SJ, Kim H-J, Cho E, et al, *Development of a membrane electrode assembly for alkaline water electrolysis by direct electrodeposition of nickel on carbon papers.* Appl Catal B: Environmental, 2014. **154**: p. 197–205.
33. Wilmer Licona Buelvas, K.C.P.Á., Álvaro Realpe Jiménez, *Temperature as a Factor Determining on WaterElectrolysis.* International Journal of Engineering Trends and Technology (IJETT) 2014. **7**(1).
34. Ibrahim dincer, c.z., *sustainable hydrogen production*. 2016: joe hayton.
35. Porciúncula, C.B., *production of hydrogen in the reaction between aluminum and water in the presence of NaOH and KOH.* Brazilian Journal of Chemical Engineering, 2012. **29**(02): p. 337-348.
36. Kim, D.K., *Performance Analysis of Polymer Electrolyte Membrane Water Electrolyzer Using OpenFOAM®:Two-Phase Flow Regime, Electrochemical Model.* Membranes, 2020. **10**: p. 441.
37. F.M.Spountzi, J.M.G., C. J. Weststrate, H. O. A. Fredresksson, J. W. Niemantsverdiet, *Electrocatalysts for the generation of hydrogen, oxygen and synthesis gas.* Energy Combust. Sci, 2017. **58**: p. 1-35.
38. Buttler A, S.H., *Current status of water electrolysis for energy storage grid balancing and sector coupling via power-to-gas and power-to-liquids: a review.* Renewable and sustainable Energy Reviews, 2018. **82**: p. 2440-2454.
39. Carmo M. Fritz DI., M.J.S.D., *A Comprehensive review on PEM water electrolysis.* Int J Hydrogen Energy 2013. **38**(12): p. 4901-4934.
40. Lehner M, T.R., Steinmuller H, Koppe M, *Power-to-gas: technology and business models*. 2014: Springer.
41. M, L.-B., *Recent advances in high temperature electrolysis using solid oxide fuel cells: a review.* J Power Sources 2012. **203**: p. 4-16.
42. Chi J, Y.H., *Water electrolysis based on renewable energy for hydrogen production.* Chin J Catal, 2018. **39**(3): p. 390-394.
43. Schmidt O, G.A., Staffell I, Hawkes A, Nelson J, Few S. , *Future cost and performance of water electrolysis an expert elicitation study.* Int J Hydrogen Energy, 2017. **42**(52): p. 30470-30492.

الملخص العربى

تم إنشاء الخلية المقترحة على شكل مهد (سرير) ثابت كما هو موضح في الشكل (1). الأقطاب الكهربائية من الفولاذ المقاوم للصدأ 316L (16-18 بالمائة كروم ، 10-14 بالمائة نيكل ، 2-3 بالمائة موليبدينوم ، 0.08 بالمائة كربون) كأسطوانات بارتفاع 15 ملم وقطرها 15 ملم مغمورة في محلول مائي من من هيدروكسيد الصوديوم كمحلول أنودى ومحلول كاثودى يتم ضخه من خزان من الفولاذ المقاوم للصدأ سعة 30 لترًا بواسطة مضختين منالبلاستيك بمعدلات تدفق مختلفة تبلغ 1 ، 2 ، 3 لترات في الدقيقة. في هذه الدراسة ، قمنا بتكبير مساحة السطح إلى 757،045 سم^2 على كل جانب واستخدمنا نفس تركيز هيدروكسيد الصوديوم عند درجات حرارة مختلفة (55 درجة مئوية ، 65 درجة مئوية ، 75 درجة مئوية) وكثافة التيار (4 ، 6 ، 8 مللي أمبير / سم^2) لزيادة كفاءة الخلية من 8.3٪ إلى 81.5٪.يعتمد مخطط هذه الدراسة على أداء الخلية من حيث تركيز المحلول ، وكثافة التيار ، ومعدل التدفق ، ودرجة الحرارة ، وقياس معدل تدفق غاز الهيدروجين الناتج (مللى / دقيقة) ، وانخفاض حجم محلول الإلكتروليت وجهد الخلية. يتم حساب كمية غاز الأكسجين الناتج ، واستهلاك الطاقة ، والقدرة المستهلكة، سعة الأمبير لكل ساعة ، ويتم حساب كفاءة الخلية من خلال مقارنة معدل التدفق الكتلي النظري والعملى لغاز الهيدروجين الناتج. بالإضافة إلى ذلك ، فتم التأكد من نقاء الغاز الناتج باستخدام الكروماتوجرافيوتوصيف الأقطاب الكهربائية باستخدام SEM ومعرفة مكونات السبيكة يضمن عدم تأثر المعدن الكاثودي بالتفاعل كما هو موضح في الشكل(2)

Table (1)

Comparison between the main characteristics in electrolysis technology

	Present work	**(ALE) Liquid /conventional electrolysis**	**(ALE) Polymeric exchange membrane**	**(PEM)Polymeric exchange membrane**	**(SOE) Solid electrolyte electrolysis**	**References**
Anode	Stainless steel 316L	Ni, Co, Fe Oxides	Ni based	IrO_2, RuO_2, TiO_2 support	Mn, Zr Oxides	[37]
Cathode	Stainless steel 316L	Ni alloy	Ni, Ni-Fe, Oxides	Pt/C, MoS_2	Ni based	[38]
Electrolyte	liquid	liquid	Solid polymeric	Solid polymeric	Solid (ceramic)	[38]
Membrane	Cation	Anion	Anion	Cation	Cation or anion	[38]
%Efficiency	8-81.5	59-70	40-80	65-82	<100	[38-40]
Cell voltage (V)	2.2-6.5	1.8-2.4	1.8-2.2	1.8-2.2	0.7-1.05	[40, 41]
Current density (A/cm^2)	0.004 - 0.008	0.2-0.4	0.6-2.0	0.6-2.0	0.3-2.0	[39, 40, 42]
Charge carrier	Na^+	OH^-	OH^-	H^+	H^+ or O^{-2}	[38]
Temperature (^0C)	55-75	20-80	20-200	20-200	500-1000	[39, 40, 42]
Applicability	commercial	commercial	Lab scale	Near commercial	Lab scale	[42, 43]
Advantages	Low cost, Stable operation	Low cost Stable operation	High purity (99.99 %), fast start up	High purity (99.99%), fast response	Low cost, High efficiency, high purity (99.99 %)	[43]

1.Stainless steel storage tank (30 liter).
2.Electric heater with temperature control.
3.Centrifuge plastic pump.
4.Digital temperature screen.
5.Liquid flow meter (L/Min) for catholyte.
6.Liquid flow meter (L/Min) for anolyte.
7.Cathodic metal (Stainless steel 316 rods).
8.Cation exchange membrane.
9.Anodic metal (Stainless steel 316 rods).
10.Stainless steel valve control catholyte flow rate.
11.Stainless steel valve control anolyte flow rate.
12.Voltammeter.
13.D.C power supply.
14.Ammeter.
15.Condenser.
16.Condenser.
17.Gas flow meter (ml/min) of evolved hydrogen gas.
18.Gas flow meter (ml/min) of evolved oxygen gas.
19.Non return valve for evolved hydrogen gas.
20.Non return valve for evolved oxygen gas.
21.Storage tank of evolved hydrogen gas.
22.Storage tank of evolved oxygen gas.
23.Pressure gauge for evolved hydrogen gas.
24.Pressure gauge for evolved oxygen gas.
25.Plastic valve to control hydrogen gas pressure.
26.Plastic valve to control oxygen gas pressure

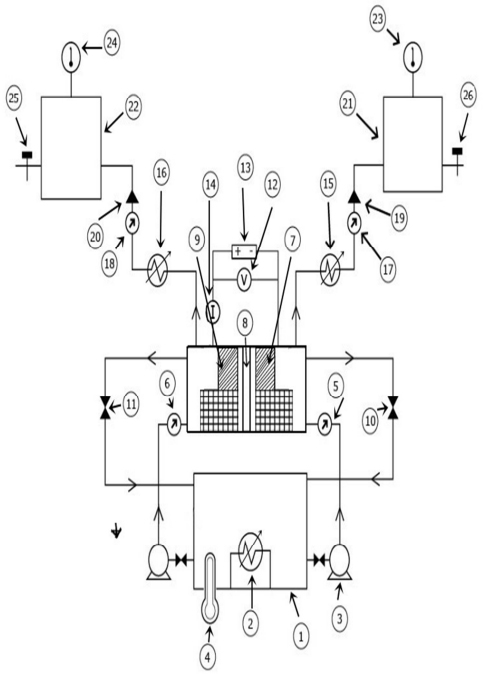

Figure (1): Schematic diagram of alkaline electrolyzer

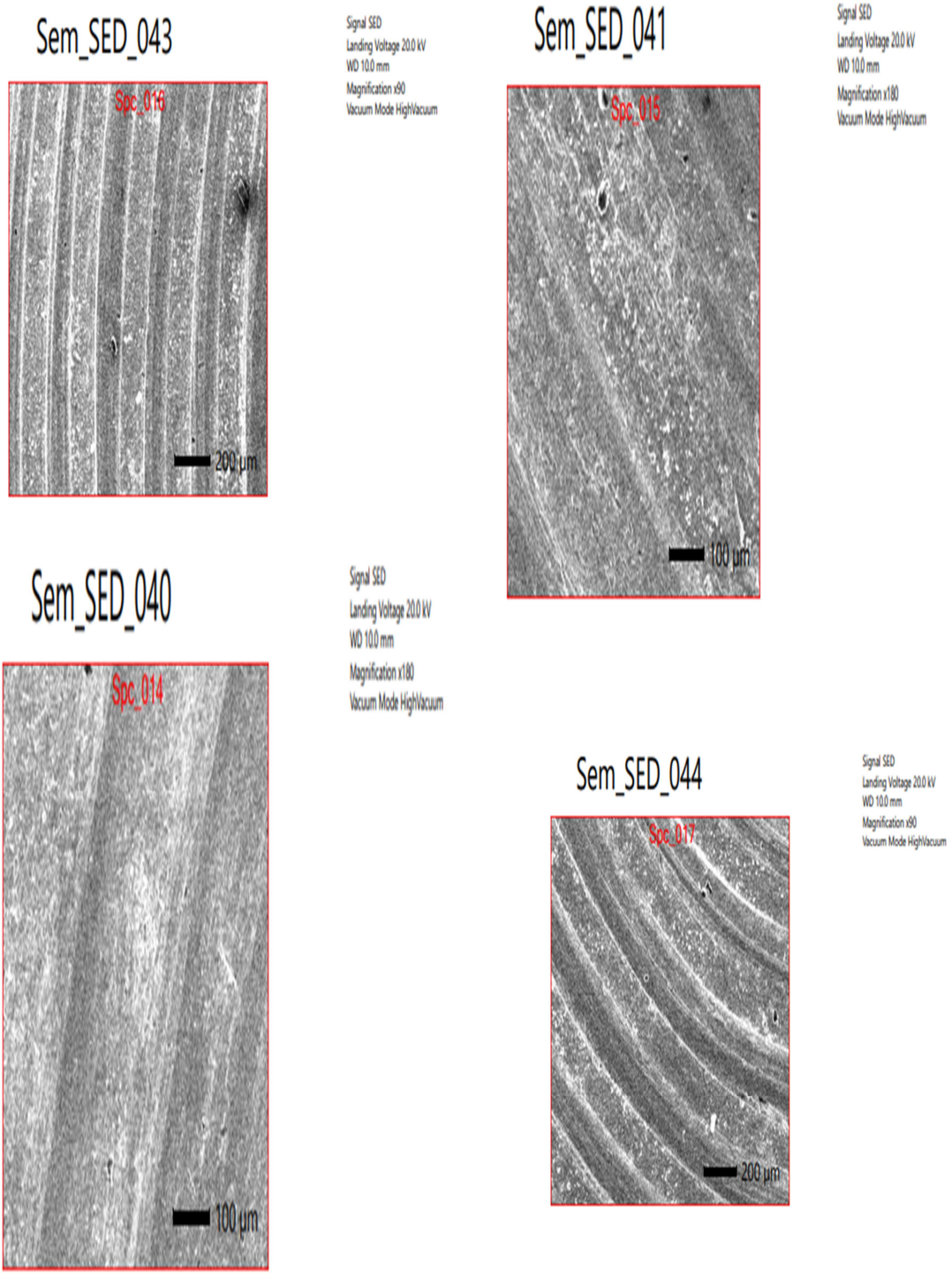

Figure (2-a): Morphological examination of the surfaces of stainless-steel rods before experiments by SEM

Figure (2-b): Morphological examination of the surfaces of stainless-steel rods after experiments by SEM

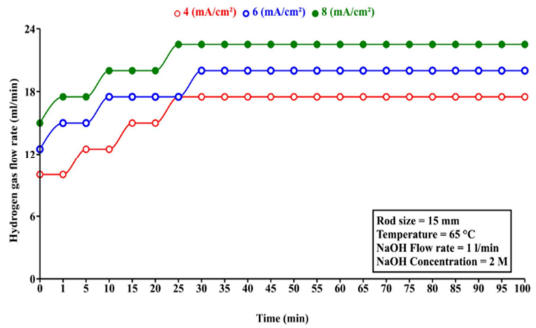

Figure (3): Hydrogen gas flow rate (ml/min) against time (min) at different current densities (mA/cm^2)

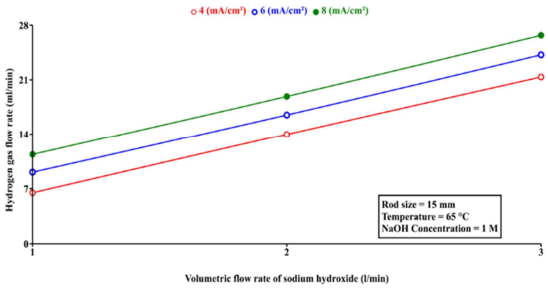

Figure (4): Hydrogen gas flow rate (ml/min) against volumetric flow rate of sodium hydroxide solution (L/min) at different current densities (mA/cm^2)

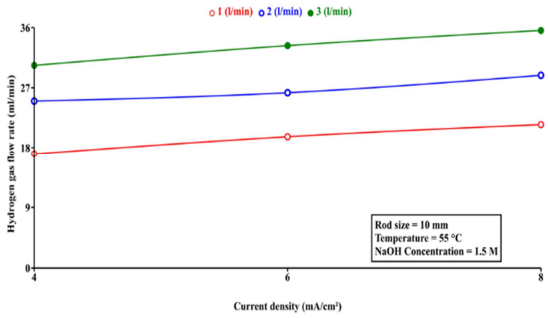

Figure (5): Hydrogen gas flow rate (ml/min) against different current densities (mA/cm^2) at different volumetric flow rate of sodium hydroxide solution (L/min)

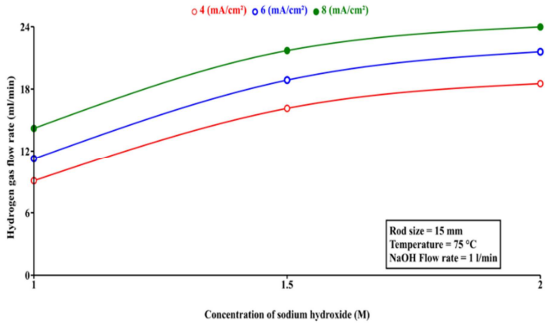

Figure (6): Hydrogen gas flow rate (ml/min) against concentration of sodium hydroxide solution (M) at different current densities (mA/cm^2)

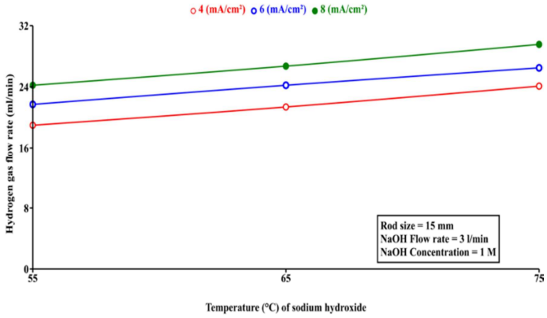

Figure (7): Hydrogen gas flow rate (ml/min) against temperature of sodium hydroxide solution (ºC) at different current densities (mA/cm^2)

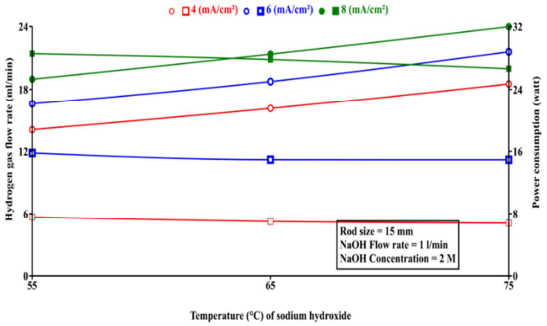

Figure (8): Hydrogen gas flow rate [O] in (ml/min) and power consumption [□] in (watt) against temperature of sodium hydroxide solution (ºC) at different current densities (mA/cm^2)

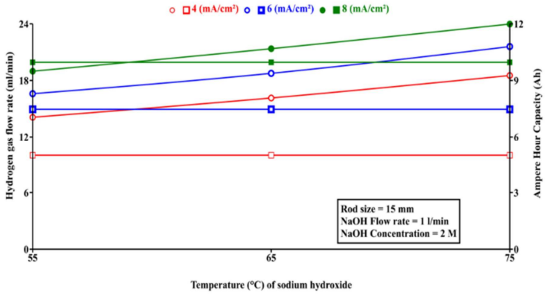

Figure (9): Hydrogen gas flow rate [O] in (ml/min) and ampere hour capacity consumption [□] in (Ah) against temperature of sodium hydroxide solution (ºC) at different current densities (mA/cm^2)

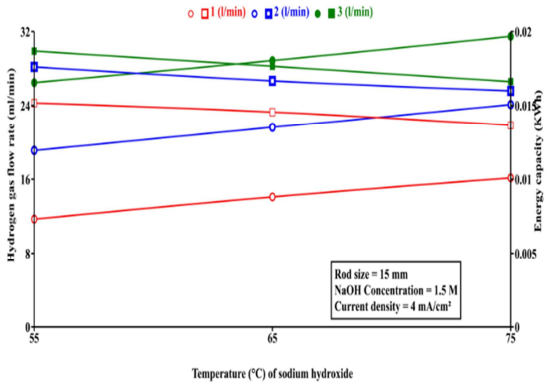

Figure (10): Hydrogen gas flow rate [O] in (ml/min) and energy capacity consumption [□] in (KWh) against temperature of sodium hydroxide solution (ºC) at different volumetric flow rate of sodium hydroxide (L/min)

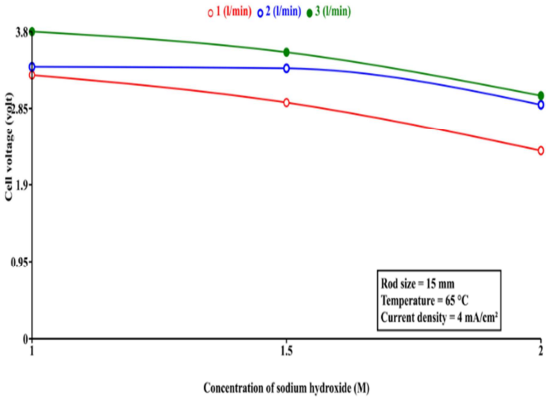

Figure (11): Cell voltage (Volts) against concentration of sodium hydroxide solution (M) at different volumetric flow rate of sodium hydroxide (L/min)

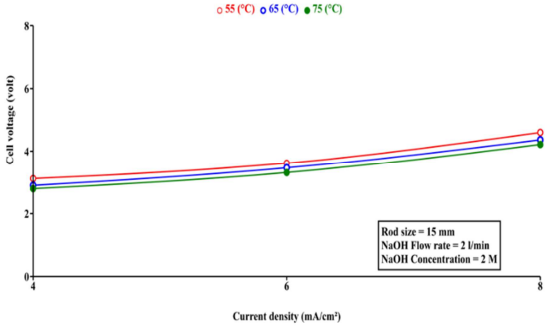

Figure (12): Cell voltage (Volts) against temperature of sodium hydroxide solution (ºC) at different concentration of sodium hydroxide solution (M)

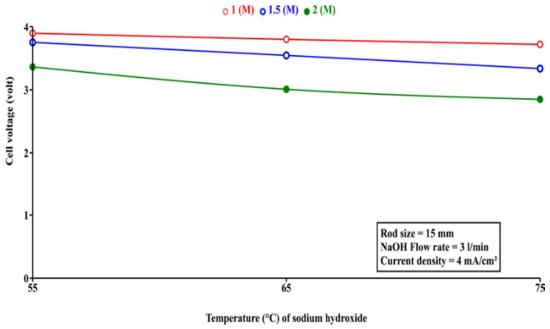

Figure (13): Cell voltage (Volts) against current density (mA/cm^2) at different temperature of sodium hydroxide solution (ºC)

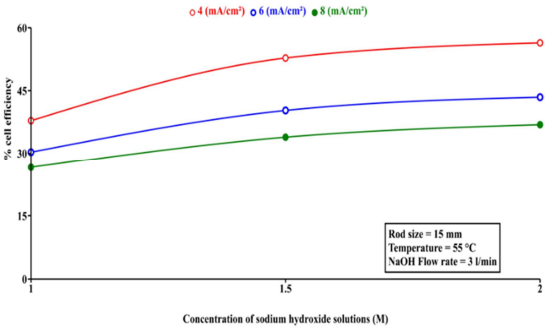

Figure (14): % Cell efficiency against concentration of sodium hydroxide solution (mole/L) at different current densities (mA/cm^2)

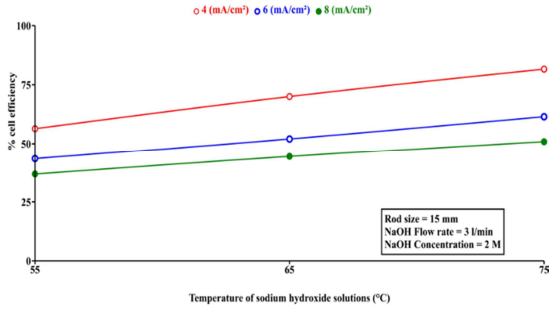

Figure (15): % Cell efficiency against temperature of sodium hydroxide solution (℃) at different current densities (mA/cm^2)

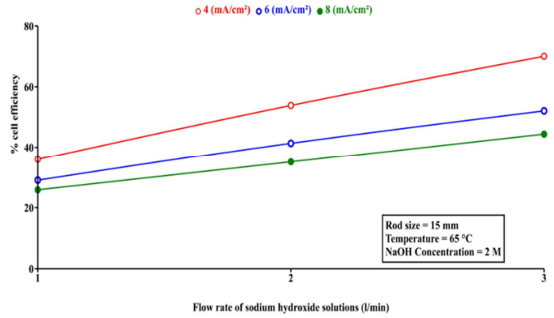

Figure (16): % Cell efficiency against volumetric flow rate of sodium hydroxide solution (L/min) at different current densities (mA/cm^2)

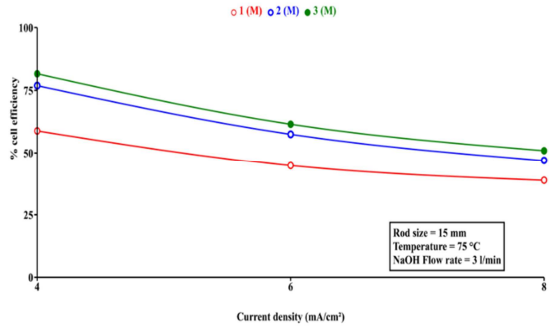

Figure (17): % Cell efficiency against current densities (mA/cm^2) at different concentration of sodium hydroxide solution (M)